Proceedings of the ASME 2015 International Mechanical Engineering Congress & Exposition
IMECE 2015
November 13-September 19, 2015, Houston, USA

IMECE2015-50094

OPTIMAL DESIGN OF SOLENOID ACTUATED BUTTERFLY VALVES DYNAMICALLY COUPLED IN SERIES

Peiman Naseradinmousavi
Assistant Professor
Department of Mechanical Engineernig
San Diego State University (SDSU)
San Diego, California 92115
Email: pnaseradinmousavi@mail.sdsu.edu

ABSTRACT

In this effort, we present novel nonlinear modeling of two solenoid actuated butterfly valves subject to a sudden contraction and then develop an optimal configuration in the presence of highly coupled nonlinear dynamics. The valves are used in the so-called "Smart Systems" to be employed in a wide range of applications including bioengineering, medicine, and engineering fields. Typically, tens of the actuated valves are instantaneously operating to regulate the amount of flow and also to avoid probable catastrophic disasters which have been observed in the practice. We focus on minimizing the amount of energy used in the system as one of the most critical design criteria to yield an efficient operation. We optimize the actuation subsystems interacting with the highly nonlinear flow loads in order to minimize a lumped amount of energy consumed. The contribution of this work is to include coupled nonlinearities of electromechanical valve systems to optimize the actuation units. Stochastic, heuristic, and gradient based algorithms are utilized in seeking the optimal design of two configurations of solenoid actuated valves. The results indicate that substantial amount of energy can be saved by an intelligent design that helps select parameters carefully but also uses flow torques to augment the closing efforts.

1 Introduction

Generally "Smart Systems" have received much attention for a wide range of applications to be operated efficiently with respect to the amount of energy used in the actuator units. The US Navy has particularly focused on developing reliable and energy efficient systems to minimize the cost of operation and also to increase crew safety through a stable performance.

Automation systems typically consist of actuators, sensors, controllers, valves, piping, electrical cabling and communication wiring. Many types of actuator-valve systems are in use [1, 2]. One of the most critical systems to be utilized in cooling purposes is the so-called "Smart Valve" system. The main objective of the smart valves is to shut down automatically in case of breakage and to reroute the flow as needed.

These sets include many interdisciplinary components interacting with each other through highly coupled nonlinear dynamics. We have previously analyzed a solenoid actuated butterfly valve dealing with electromagnetics and fluid mechanics [3–6]. High fidelity mathematical models were developed for both the single and coupled actuated valves. For the single set [3], our focus was on developing a nonlinear model to analyze the complicated physics of the system to be used in dynamic analysis [4] and optimization. [5]

We have captured transient chaotic and crisis dynamics of the single valve actuator for some critical parameters helping to define the safe domain of operation. Determining the safe operational domain through the stability map helped us define the lower and upper bounds of the optimization tasks [5] and operation, which reduced the amount of energy used in the single set. The first phase was to optimize the system design, particularly the actuation unit coupled with the mechanical and fluid parts. We then optimized the valve operation to be closed in an efficient

fashion yielding the minimum energy consumption. In both the optimization schemes, the roles of flow torques are important to help close the valve with minimal energy.

It is of great interest to emphasize that the smart valve systems contain many of the actuated sets and hence, they would not be independent of each other. These dependencies have been observed in the practice and probable malfunction of each set may expectedly result in the catastrophic behavior of the whole system. Therefore, we have developed the coupled dynamic model of two actuated valves operating in series [6]. A periodic noise was applied on the upstream valve to evaluate its effects on the downstream set of the valve and actuator. A powerful tool of the nonlinear dynamic analysis (power spectrum) was then employed to present the same oscillatory response of the downstream set with that of the upstream one; as expected, the downstream set revealed the same frequencies of response with a smaller amplitude. Any slight dynamic change of the upstream set, on the other hand, was shown to be effective for the downstream set through the media trapped between two valves.

Capturing the coupled dynamics of two actuated valves would help us optimize the design of both the actuation units in which an interesting connection can be distinguished between the currents. The currents are subject to the interconnected flow torques and pressure drops of the valves. Note that, for the single set, we neglected the interactions among the actuators/valves operating in series although the magnetic parts are remarkably affected by the dynamics of the neighbor sets [6].

Optimization of solenoid actuators has recently received some attention. Ju and Woong [7] have focused on the optimal design of solenoid actuators using a non-magnetic ring. Electromagnetic actuator-current development has been carried out by Hameyer and Nienhaus [8], and Sung *et al*. [9] studied development of a design process for on-off type of solenoid actuators. Kajima [10] has considered a dynamic model of the plunger type of solenoids. Karr and Scott [11] utilized the genetic algorithm to optimize an anti-resonant electromechanical controller operating in frequency domain. Mahdi [12] carried out optimization of the PID controller parameters to operate nonlinear electromechanical actuator efficiently. A coupled electromechanical optimization of the cost of high speed railway overheads has been carried out by Jimenez-Octavio *et al.* [13]. Nowak [14] has focused on presenting an algorithm of the optimization of the dynamic parameters of an electromagnetic linear actuator operating in error-actuated control system. Other contributions in design optimization of electromechanical actuators include [15–21].

This paper begins with a brief nonlinear dynamic model of the actuators/valves operating in series but slightly different from the model reported in [6] due to the sudden contraction. In the practice, multiple contractions and expansions exist through the pipeline. The coupled modeling and then analysis of these configurations would hence be necessary to capture highly nonlinear mutual interactions among the sets. Then, the optimal design process is formulated to help select the efficient actuators' parameters coupled with the electromagnetical, mechanical, and fluid parts in order to yield an energy efficient system. Most electromechanical systems used in the flow control lines have been studied by neglecting the interconnections imposed by other sets. From another aspect, the linearization method, as one of the simplest practices, is widely being utilized in many of analytical investigations particularly for the systems with a higher level of complexity and coupling. The results of both the isolated- and linearized analyses may expectedly be valid within a narrow domain of operation leading typically to significant inaccuracy and unreliability of the results. The contribution of this work is to optimize both the actuated valves dynamically coupled in different aspects while our previous effort [5] was on optimizing a single unit by neglecting its dynamic coupling with another set. A considerable amount of energy saving was obtained via the isolated analysis but would obviously could be affected by the dynamic interactions among sets. In this effort, a lumped cost function will be minimized, with respect to the stability and physical constraints, using global optimization tools in order to obtain efficient design and operation of the actuation units and valves, respectively. This would provide an interesting opportunity to utilize the coupled optimization scheme, which is being developed here, for other large-scale networks including oil and gas fields, municipal piping systems, petrochemical plants, and aerospace. The need for optimization clearly exists for such networks in order to improve efficiency.

2 Mathematical Modeling

The system being optimized consists of two solenoid actuated butterfly valves operating in series as shown in Fig. 1(a). The actuators are connected to the valves' stems through the rack and pinion arrangements. Applying electric voltages (AC or DC), the magnetic forces move the plungers and consequently rotate both the valves to desirable angles. Note that we utilize a return spring to open the valves; this is a common practice among manufacturers.

The mathematical modeling of such a coupled system obviously needs some simplifying assumptions to avoid useless and cumbersome numerical calculations. The first one is to neglect the magnetic diffusion. During the diffusion time, there is no powerful magnetic force to move the plunger and the valve subsequently would not rotate in that time interval. Note that the diffusion time has an inverse relationship with the amount of current [3] such that a large value of the current yields a negligible diffusion time and vice versa. We apply a current of $i = 13(A)$ for both the actuators yielding the diffusion time of $\tau_d \approx 6(ms)$ which can be easily neglected considering the nominal operation time.

The second assumption is to utilize laminar flow for both the valves. This is a common practice to avoid the tedious nu-

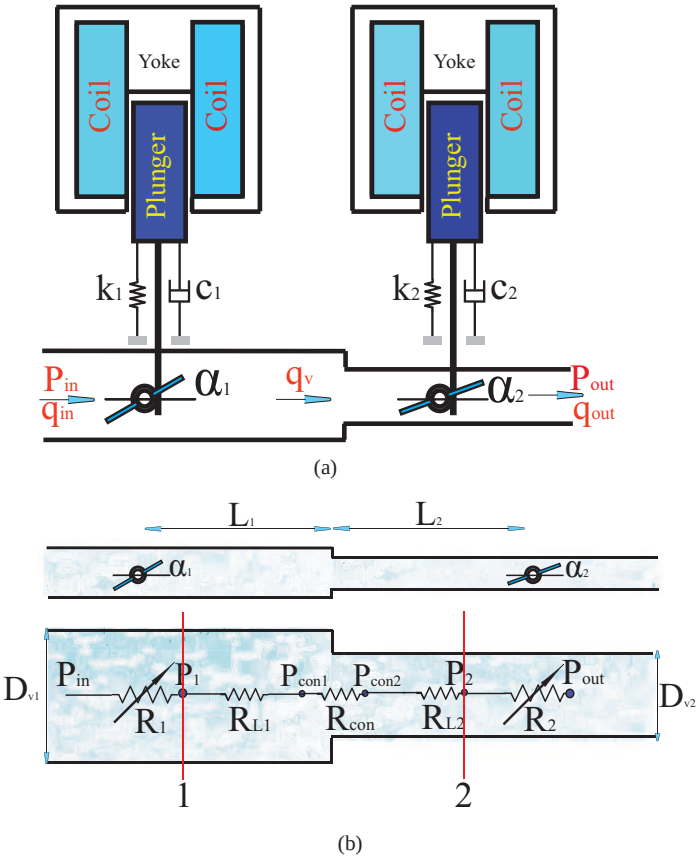

FIGURE 1. (a) Two actuated butterfly valves subject to the sudden contraction; (b) A model of two valves in series without actuation

merical calculations of a turbulent regime and also to develop an analytical model to be used in the nonlinear dynamic analysis. The dynamic analysis needs to be done to capture the dangerous responses of the system [4]. The validity of laminar flow assumption needs to be examined particularly with respect to the amounts of inlet velocity and pipe diameter given in Table 1. Using these values, the Reynolds number indicates the existence of the turbulent regime and questions the assumption of laminar flow. We hence carried out experimental work shown in Fig. 2 to examine the validity of the assumption. Shown in Fig. 3 is the total torque, sum of both the hydrodynamic and bearing ones, for the inlet velocity of $V_0 \approx 2.7\left(\frac{m}{s}\right)$ and valve diameter of $D_v = 2\ (inches)$ revealing an acceptable consistency [22] among the experimental data and the formula utilized in the analytical studies based on the laminar flow. This also gives us the confidence to use the analytically (and computationally) derived mathematical expressions for the hydrodynamic and bearing torques. We previously discussed the important roles of both the torques on the dynamic response of a single actuated valve and subsequently such effects are expected to be observed for

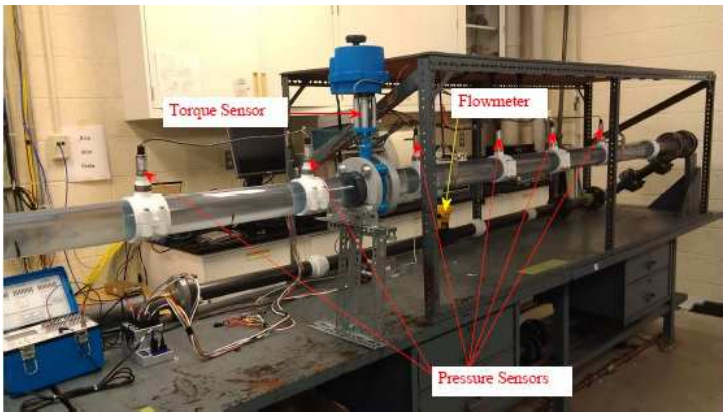

FIGURE 2. The experimental work carried out for a single set

TABLE 1. The system parameters

ρ	$1000\frac{kg}{m^3}$	v	$3\frac{m}{s}$
μ	0.5	P_{in}	256(kPa)
$J_{1,2}$	$0.104\times10^{-1}(kg.m^2)$	$b_{d1,d2}$	$10^3\frac{N.m.s}{rad}$
$N_{1,2}$	3300	$C_{11,12}$	$1.56\times10^6(H^{-1})$
$g_{m1,m2}$	0.1(m)	$V_{1,2}$	24(Volt)
D_{v1}	8(in)	D_{v2}	5(in)
$D_{s1,s2}$	0.5(in)	P_{out}	2(kPa)
$k_{1,2}$	60(N.m)	$C_{21,22}$	$6.32\times10^8(H^{-1})$
L_1	$2(m)$	L_2	$1(m)$
μ_f	$0.018\ (Kg.m^{-1}.s^{-1})$	$R_{1,2}$	$1.8(\Omega)$
$r_{1,2}$	0.05(m)	θ	90°

the coupled sets [6].

We modeled the coupled system as two changing resistors for the opening/closing valves plus three constant ones in the middle of the valves, shown in Fig. 1(b). Two of the constant resistors stand for head losses and another one is due to the sudden contraction. The inlet and outlet pressures are supposed to be known. Applying the assumption stated for the dominant laminar flow, the Hagen-Poiseuille [23] and Borda-Carnot [24] formulas express the pressure drops between two valves (points 1 and 2):

$$P_1 - P_{con1} = \underbrace{\frac{128\mu_f L_1}{\pi D_{v1}^4}}_{R_{L1}} q_v \qquad (1)$$

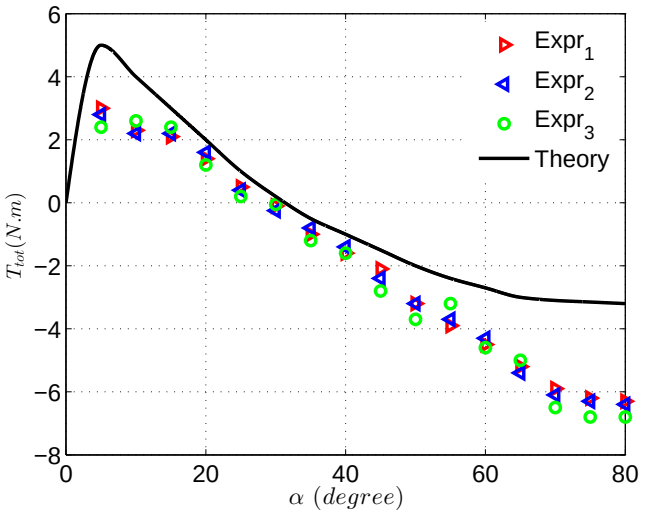

FIGURE 3. The experimental and analytical total torques for the inlet velocity of $V_0 \approx 2.7\left(\frac{m}{s}\right)$ and valve diameter of $D_v = 2\ (inches)$

$$P_{con1} - P_{con2} = \frac{1}{2} K_{con} \rho v_{out}^2 \tag{2}$$

$$P_{con2} - P_2 = \underbrace{\frac{128 \mu_f L_2}{\pi D_{v2}^4}}_{R_{L2}} q_v \tag{3}$$

where, μ_f is the fluid dynamic viscosity, D_{v1} and D_{v2} stand for the valves' diameters, q_v indicates the volumetric flow rate, L_1 and L_2 are the pipe lengths before and after contraction, P_{con1} and P_{con2} indicate the flow pressures before and after contraction, and R_{L1} and R_{L2} are the constant resistances. K_{con} is easily calculated as follows.

$$K_{con} = 0.5(1-\beta^2)\sqrt{\sin\left(\frac{\theta}{2}\right)} \tag{4}$$

where, θ is the angle of approach and β indicates the ratio of minor and major diameters $\left(\frac{D_{v2}}{D_{v1}}\right)$. Using the parameters given in Table 1, we obtain $K_{con} = 0.2562$. We rewrite Eq. 2 as the following:

$$\begin{aligned} P_{con1} - P_{con2} &= \frac{1}{2} K_{con} \rho v_{out}^2 \\ &= \underbrace{\frac{8 K_{con}}{\pi^2 D_{v2}^4} \rho}_{R_{con}} \underbrace{\frac{\pi^2 D_{v2}^4 v_{out}^2}{16}}_{q_v^2} \\ &= R_{con} q_v^2 \end{aligned} \tag{5}$$

where, R_{con} is the resistance due to the sudden contraction. Adding Eqs. 1,2, 3, and 5 easily yields,

$$P_1 - P_2 = [R_{L1} + R_{L2} + R_{con} q_v] q_v \tag{6}$$

The valve's "Resistance (R)" and "Coefficient (c_v)" are the most important parameters of the regulating valves including butterfly ones. The valve's resistance and coefficient are nonlinear functions of the valve rotation angle [25]:

$$R_i(\alpha_i) = \frac{891 D_{vi}^4}{c_{vi}^2(\alpha_i)},\ i = 1,2 \tag{7}$$

The pressure drop across the valve is stated as follows [26]:

$$\Delta P_i(\alpha_i) = 0.5 R_i(\alpha_i) \rho v^2 \tag{8}$$

where, α indicates the valve rotation angle, v is the flow velocity, and ρ stands for the density of the media. Rewriting Eq. 8 yields,

$$\Delta P_i(\alpha_i) = \underbrace{\frac{\pi^2 D_{vi}^4 v^2}{16}}_{q_v^2} \underbrace{\frac{8 \times R_i(\alpha_i) \rho}{\pi^2 D_{vi}^4}}_{R_{ni}(\alpha_i)} = R_{ni}(\alpha_i) q_v^2 \tag{9}$$

We established that both the hydrodynamic (T_h) and bearing (T_b) torques [26, 27] are too sensitive to the pressure drop obtained via Eq. 9 leading us to reformulate them to be stated as follows.

$$f_i(\alpha_i) = \frac{16 T_{ci}(\alpha_i)}{3\pi\left(1 - \frac{C_{cci}(\alpha_i)(1-\sin(\alpha_i))}{2}\right)^2} \tag{10}$$

$$T_{hi} = \frac{16 T_{ci}(\alpha_i) D_{vi}^3 \Delta P_i}{3\pi\left(1 - \frac{C_{cci}(\alpha_i)(1-\sin(\alpha_i))}{2}\right)^2} = f_i(\alpha_i) D_{vi}^3 \Delta P_i \tag{11}$$

$$T_{bi} = 0.5 A_d \Delta P_i \mu D_s = C_i \Delta P_i \tag{12}$$

where, μ is the friction coefficient of the bearing area, D_s indicates the stem diameter of the valve, $C_i = \frac{\pi}{8} \mu D_{vi}^2 D_s$, and T_{ci} and C_{cci} stand for the hydrodynamic torque and the sum of upper and lower contraction coefficients, respectively; they depend on the valve rotation angle [3].

The nonlinear dynamic analysis carried out for a set of the actuator/valve [4] provides the criteria needed to determine the bounds of the optimization tasks; the stability analysis obviously needs to be done using an analytical model. The same practice we would utilize for the coupled system with the aid of fitting suitable curves on c_{vi} and R_{ni} in order to model the system analytically. For our case study of D_{v1}=8 (in) and D_{v2}=5 (in), the valves' coefficients and resistances are formulated as follows.

$$c_{v1}(\alpha_1) = p_1\alpha_1^3 + q_1\alpha_1^2 + o_1\alpha_1 + s_1 \tag{13}$$

$$c_{v2}(\alpha_2) = p_2\alpha_2^3 + q_2\alpha_2^2 + o_2\alpha_2 + s_2 \tag{14}$$

$$R_{n1}(\alpha_1) = \frac{e_1}{(p_1\alpha_1^3 + q_1\alpha_1^2 + o_1\alpha_1 + s_1)^2} \tag{15}$$

$$R_{n2}(\alpha_2) = \frac{e_2}{(p_2\alpha_2^3 + q_2\alpha_2^2 + o_2\alpha_2 + s_2)^2} \tag{16}$$

where, $e_1 = 7.2\times10^5$, $e_2 = 4.51\times10^5$, $p_1 = 461.9$, $p_2 = 161.84$, $q_1 = -405.4$, $q_2 = -110.53$, $o_1 = -1831$, $o_2 = -695.1$, $s_1 = 2207$, and $s_2 = 807.57$. Clearly the mass continuity principle implies $q_{in} = q_{out} = q_v$. Rewriting Eq. 9 then yields,

$$\frac{P_{in} - P_1}{R_{n1}(\alpha_1)} = \frac{P_2 - P_{out}}{R_{n2}(\alpha_2)} \tag{17}$$

$$R_{n1}P_2 + R_{n2}P_1 = R_{n2}P_{in} + R_{n1}P_{out} \tag{18}$$

One can easily derive the coupled P_1 and P_2 terms by combining Eqs. 6 and 18 as follows:

$$P_1 = \frac{R_{n2}P_{in} + R_{n1}P_{out} + R_{n1}(R_{L1} + R_{L2} + R_{con}q_v)q_v}{(R_{n1} + R_{n2})} \tag{19}$$

$$P_2 = \frac{R_{n2}P_{in} + R_{n1}P_{out} - R_{n2}(R_{L1} + R_{L2} + R_{con}q_v)q_v}{(R_{n1} + R_{n2})} \tag{20}$$

Eqs. 19 and 20 state the roles of R_{n1}, R_{n2}, R_{L1}, R_{L2}, and R_{con} on the variations of P_1 and P_2 with the given values of P_{in}, P_{out}, and q_v, as observed in the practice. Therefore, it is fairly straightforward to conclude the dynamic sensitivity of the downstream set to any slight changes of the upstream one. We then can rewrite both the hydrodynamic and bearing torques dependency on all the resistances as follows.

$$T_{hi} = f_i(\alpha_i)D_{vi}^3\Delta P_i(R_{n1}, R_{n2}, R_{L1}, R_{L2}, R_{con}) \tag{21}$$

$$T_{bi} = C_i\Delta P_i(R_{n1}, R_{n2}, R_{L1}, R_{L2}, R_{con}) \tag{22}$$

Note that f_i is a function of many nonlinear terms which include the changing T_{ci} and C_{cci} in addition to the valves' angles. For a systematic analysis of the whole system, the following functions are fitted to the $D_{vi}^3 f_i$ of each valve:

$$\begin{aligned} T_{h1} &= \underbrace{(a_1\alpha_1 e^{b_1{\alpha_1}^{1.1}} - c_1 e^{d_1\alpha_1})}_{D_{v1}^3 f_1}(P_{in} - P_1) \\ &= (a_1\alpha_1 e^{b_1{\alpha_1}^{1.1}} - c_1 e^{d_1\alpha_1}) \times \frac{\frac{e_1}{(p_1\alpha_1^3 + q_1\alpha_1^2 + o_1\alpha_1 + s_1)^2}}{\sum_{i=1}^{2}\frac{e_i}{(p_i\alpha_i^3 + q_i\alpha_i^2 + o_i\alpha_i + s_i)^2}} \\ &\times (P_{in} - P_{out} - (R_{L1} + R_{L2} + R_{con}q_v)q_v) \end{aligned} \tag{23}$$

$$\begin{aligned} T_{h2} &= \underbrace{(a_1'\alpha_2 e^{b_1'\alpha_2^{1.1}} - c_1' e^{d_1'\alpha_2})}_{D_{v2}^3 f_2}(P_2 - P_{out}) \\ &= (a_1'\alpha_2 e^{b_1'{\alpha_2}^{1.1}} - c_1' e^{d_1'\alpha_2}) \times \frac{\frac{e_2}{(p_2\alpha_2^3 + q_2\alpha_2^2 + o_2\alpha_2 + s_2)^2}}{\sum_{i=1}^{2}\frac{e_i}{(p_i\alpha_i^3 + q_i\alpha_i^2 + o_i\alpha_i + s_i)^2}} \\ &\times (P_{in} - P_{out} - (R_{L1} + R_{L2} + R_{con}q_v)q_v) \end{aligned} \tag{24}$$

where, $a_1 = 0.4249$, $a_1' = 0.1022$, $b_1 = -18.52$, $b_1' = -17.0795$, $c_1 = -7.823\times10^{-4}$, $c_1' = -2\times10^{-4}$, $d_1 = -1.084$, and $d_1' = -1.0973$. We also replace the sign function ($sign(\dot{\alpha}_i)$), which is being used in the bearing torque statement to present its resistance role, by the smooth function $\tanh(K\dot{\alpha}_i)$ for ease of analysis. Figs. 4(a) and 4(b) are results of the stability analysis of the coupled system; we will report this effort as another article.

The state variables are defined as follows.

$$[z_1, z_2, z_3, z_4, z_5, z_6 = \alpha_1, \dot{\alpha}_1, i_1, \alpha_2, \dot{\alpha}_2, i_2]$$

We previously developed the magnetic force and rate of current terms [3] to be used in deriving the state space equations as follows.

$$F_{mi} = \frac{C_{2i}N_i^2 i_i^2}{2(C_{1i} + C_{2i}(g_{mi} - x_i))^2} \tag{25}$$

$$\begin{aligned} \frac{di_i}{dt} &= \frac{(V_i - R_i i_i)(C_{1i} + C_{2i}(g_{mi} - x_i))}{N_i^2} \\ &- \frac{C_{2i}i_i\dot{x}_i}{(C_{1i} + C_{2i}(g_{mi} - x_i))} \end{aligned} \tag{26}$$

$$\dot{z}_1 = z_2 \tag{27}$$

$$\begin{aligned} \dot{z}_2 = \frac{1}{J_1}\Bigg[&\frac{r_1 C_{21}N_1^2 z_3^2}{2(C_{11} + C_{21}(g_{m1} - r_1 z_1))^2} - b_{1d}z_2 - k_{1t}z_1 \\ &\frac{\frac{(P_{in} - P_{out} - (R_{L1} + R_{L2} + R_{con}q_v)q_v)e_1}{(p_1 z_1^3 + q_1 z_1^2 + o_1 z_1 + s_1)^2}}{\sum_{i=1,4}\frac{e_i}{(p_i z_i^3 + q_i z_i^2 + o_i z_i + s_i)^2}} \times \\ &\Big[(a_1 z_1 e^{b_1{z_1}^{1.1}} - c_1 e^{d_1 z_1}) - C_1 \times \tanh(Kz_2)\Big]\Bigg] \end{aligned} \tag{28}$$

$$\dot{z}_3 = \frac{(V_1 - R_1 z_3)(C_{11} + C_{21}(g_{m1} - r_1 z_1))}{N_1^2} -$$

$$\frac{C_{21}z_3z_2}{(C_{11}+C_{21}(g_{m1}-r_1z_1))} \tag{29}$$

$$\dot{z}_4 = z_5 \tag{30}$$

$$\dot{z}_5 = \frac{1}{J_2}\left[\frac{r_2C_{22}N_2^2z_6^2}{2(C_{12}+C_{22}(g_{m2}-r_2z_4))^2} - b_{2d}z_5 - k_{2t}z_4 \right.$$
$$\frac{\frac{(P_{in}-P_{out}-(R_{L1}+R_{L2}+R_{con}q_v)q_v)e_2}{(p_2z_4^3+q_2z_4^2+o_2z_4+s_2)^2}}{\sum_{i=1,4}\frac{e_i}{(p_iz_i^3+q_iz_i^2+o_iz_i+s_i)^2}} \times$$
$$\left.\left[(a_1'z_4e^{b_1'z_4{}^{1.1}} - c_1'e^{d_1'z_4}) - C_2\times\tanh(Kz_5)\right]\right] \tag{31}$$

$$\dot{z}_6 = \frac{(V_2-R_2z_6)(C_{12}+C_{22}(g_{m2}-r_2z_4))}{N_2^2} -$$
$$\frac{C_{22}z_5z_6}{(C_{12}+C_{22}(g_{m2}-r_2z_4))} \tag{32}$$

where, x indicates the plunger displacement, r is the radius of the pinion, F_m stands for the motive force, C_1 and C_2 are the reluctances of the magnetic path without airgap and airgap, respectively, N is the number of coils, i indicates the applied current, g_m is the nominal airgap, J is the polar moment of inertia of the valve's disk, b_d is the equivalent torsional damping, K_t indicates the equivalent torsional stiffness, V is the supply voltage, and R indicates the electrical resistance of coil. Note that K=1 resulted in a good approximation to the sign function. Eqs. 27-32 constitute the sixth order dynamic model of the coupled actuators/valves.

3 Optimal Design

Efficient optimization schemes are needed to be utilized in minimizing the amount of energy used by the whole system with respect to the stability criteria we developed earlier [4, 28]. Neglecting the parameters' constraints established through the stability analysis would result in the failure of the whole system shown in Fig. 4(a) revealing the hyperchaotic dynamics of both the valves/actuators for a set of the critical parameters; two positive Lyapunov exponents shown in Fig. 4(b) confirm the hyperchaotic behavior of the system. We selected critical values of the equivalent viscous damping and friction coefficient of the bearing area ($b_{di} = 10^{-3}$, $\mu_i = 5\times10^{-2}$), based on the stability analysis, to present the hyperchaotic dynamics of both the valves and actuators. The detailed results and discussions will be presented as another article. The US Navy has experienced such a disaster by running the flow line within the critical parameters due to the military incident.

The problem is one of constrained optimization with possibly several local minima. Therefore, we need to utilize efficient optimization approaches to get the global minimum; the constraints are the stability and physical ones. The cost function we wish to minimize is a lumped term of the energy used in both

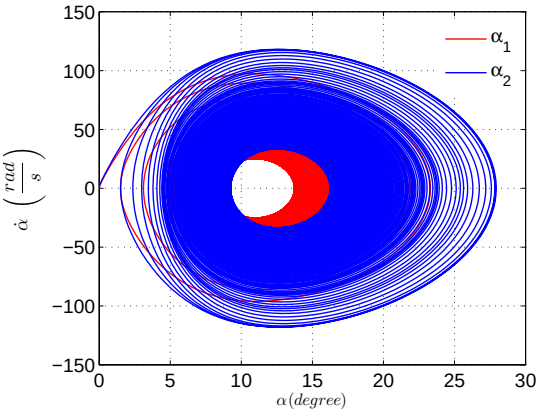

(a)

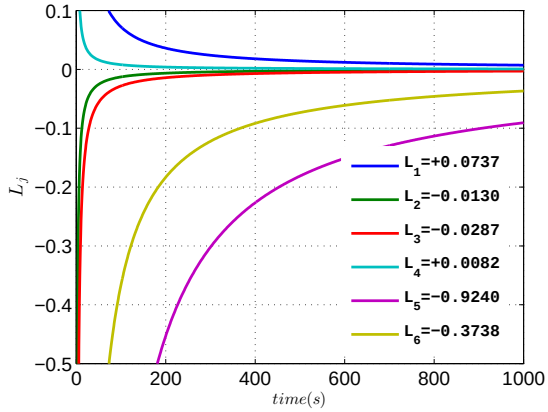

(b)

FIGURE 4. (a) The hyperchaotic dynamics of the valves/actoators; (b) The Lyapunov exponents indicating the hyperchaotic dynamics of the system

the sets.

$$\min E = \sum_{i=1}^{2}\int_0^{t_f} Vi_i\,dt \tag{33}$$
$$\text{subject to}: z_1 < 90^\circ,\ z_4 < 90^\circ$$

We previously reported that the analytical model would not be valid at $z_1 = 90^\circ$ and $z_4 = 90^\circ$ [3–6, 26]. The cost function is typically determined with respect to the scale and performance of the network. Tens of such actuated valves are used in the US Navy fleet and a lower lumped amount of energy consumed in the network is needed to reduce the cost of operation. This would lead us to select a lumped cost function to be minimized. After selecting some of the parameters as predetermined, the design variables to be used in the optimization process are chosen as follows: C_{11}, C_{12}, C_{21}, and C_{22} are the magnetic reluctances, g_{m1}

and g_{m2} indicate the airgaps, and N_1 and N_2 are the number of coils for both the actuators.

We hence define the design variables as the following:

$$\theta = [C_{11}, C_{12}, C_{21}, C_{22}, N_1, N_2, g_{m1}, g_{m2}]^T \tag{34}$$

The state equations, as discussed earlier, need to be satisfied at all times during the optimization process and the design variables are subject to the following lower and upper bounds.

$$\theta_{min} = [0.8e6, 0.8e6, 4e8, 4e8, 2900, 2900, 0.08, 0.08]^T \tag{35}$$

$$\theta_{max} = [2e6, 2e6, 9e8, 9e8, 3400, 3400, 0.11, 0.11]^T \tag{36}$$

These bounds were established based on practical system considerations, stability analysis, and physical constraints. We employ three global optimization tools including simulated annealing, genetic, and gradient based (GlobalSearch) algorithms to provide a clear map of optimization efforts with respect to the locality/globality of the cost function minima.

The first method (SA) was independently developed by Kirkpatrick *et al.* [29] and by Cerny [30]. The second one (GA) has been designed based on a heuristic search to mimic the process of natural selection [31].

One of the advantages of the simulated annealing procedure is to select a new point randomly. We hence need to set the initial guesses as random numbers. The algorithm covers all new points to reduce the objective. At the same time, with a certain probability, points that increase the objective are also accepted. The algorithm avoids to be trapped in local minima by using points that raise the objective and has the potential to search globally for more possible solutions.

The genetic algorithm is significantly more robust than other conventional ones. It does not break easily in the presence of slight changes of inputs, and noise. For a large state-space, the algorithm may potentially exhibit significantly better performance than typical optimization techniques.

The design variables in practice are not of the same order, and caused serious numerical errors in our initial studies. We solved this issue by conditioning them using a normalization scheme as follows.

$$N_{ni} = \frac{N_i}{10^3}; C_{1in} = \frac{C_{1i}}{10^6}; C_{2in} = \frac{C_{2i}}{10^8}; g_{min} = 10 g_{mi}$$

Note that random initial guesses we also used in the optimization process (as required by simulated annealing) as follows.

$$\theta_{nr} = \theta_{lb} + (\theta_{ub} - \theta_{lb}) \times \text{rand}(0,1) \tag{37}$$

where rand(0,1) is a random number between zero and one. We developed the algorithm in MATLAB and captured many interesting results.

4 Results

The predetermined parameters given in Table 1 were obtained from the experimental work we have done for the single set as shown in Fig. 2. Table 2 gives the optimal design variables utilizing the GlobalSearch, genetic, and simulated annealing algorithms. The GS, genetic, and SA algorithms terminate after 6000, 1040, and 24000 iterations, respectively, satisfying the tolerances defined for both the variables and the lumped cost function. All methods yield lower values of C_{11}, C_{12}, C_{21}, C_{22}, g_{m1}, and g_{m2}, and higher values for the number of coils with respect to their corresponding nominal values.

These optimal variables to be used in the actuation parts are considerably more efficient in that higher and lower values of the actuation forces and currents are obtained as shown in Figs. 5 and 6, respectively. Note that for both the nominal and optimal configurations, the downstream actuators' currents and forces are lower and higher, respectively, than those of the upstream ones, particularly for the optimal sets. This can be easily addressed with respect to the sudden contraction between the valves. The change of pipe diameter would potentially yield higher values of both the hydrodynamic and bearing torques acting on the downstream valve based on Eqs. 7-9, 21, and 22, to be stated as follows.

$$\frac{T_{h2}}{T_{h1}} \propto \left(\frac{D_{v2}}{D_{v1}}\right)^3 \times \left(\frac{c_{v1}}{c_{v2}}\right)^2 \tag{38}$$

$$\frac{T_{b2}}{T_{b1}} \propto \left(\frac{D_{v2} c_{v1}}{D_{v1} c_{v2}}\right)^2 \tag{39}$$

The downstream set is hence expected, for both the nominal and optimal cases, to be subject to the higher hydrodynamic and bearing torques for the approximate ranges of $0 \leq \alpha_i \leq 60^\circ$ and $\alpha_i \geq 60^\circ$, respectively, as shown in Fig. 7. From another aspect, we previously established the important roles of both the hydrodynamic and bearing torques on the valve motions. The hydrodynamic torque is a helping load to push the valve to be closed and is typically effective for when the valve angle is lower than 60° [6]. Note that the bearing torque is a resistance load and remarkably becomes effective for the valve's angle higher than that of 60°; we validated the effective ranges experimentally [6] which indicate the helping and resisting natures of the hydrodynamic and bearing torques by presenting positive and negative values, respectively. Consequently, the higher helping loads would lead to the downstream valves' higher rotation angles than those of the upstream ones, shown in Fig. 8; $\alpha_{1no} = 22^\circ$, $\alpha_{2no} = 26^\circ$, $\alpha_{1op} = 63^\circ$, and $\alpha_{2op} = 75^\circ$. The higher rotation angles minimize the dominator of the magnetic force term stated in Eq. 25 and one is expectedly able to notice slightly higher value of the force for the nominal downstream set and considerably higher amount for the optimal one in addition to the effects of the optimal design variables.

TABLE 2. The nominal and optimal variables

	Nominal	GS	GA	SA
$\frac{C_{11}}{10^6}(H^{-1})$	1.56	0.8	0.8	0.8014
$\frac{C_{21}}{10^8}(H^{-1})$	6.32	3.8	3.8009	3.8
$\frac{C_{12}}{10^6}(H^{-1})$	1.56	0.9	0.8220	0.813
$\frac{C_{22}}{10^8}(H^{-1})$	6.32	4	3.8676	3.8018
N_1	3300	3400	3398	3400
N_2	3300	3400	3330	3399
$g_{m1}(m)$	0.1	0.08	0.08	0.08
$g_{m2}(m)$	0.1	0.08	0.08	0.08
E_{tot}	25165	20563	20572	20400

The optimal design variables which include smaller values of C_{1i}'s, C_{2i}'s, g_m's and higher values of N_i's would also remarkably help magnify the magnetic forces based on Eq. 25. From another aspect, the circled area shown in Fig. 7 confirms the reduced bearing torques of the optimal sets than those of the nominal ones to help consume lower values of the currents and lumped energy. Significantly smaller amounts of currents are used in the optimal sets, as shown by the circled area in Fig. 6; this can be related to the decreased resistance torques (the bearing ones) in addition to the increased magnetic forces. Subsequently, we would be able to apply a lower level of the lumped energy to carry out the closing efforts.

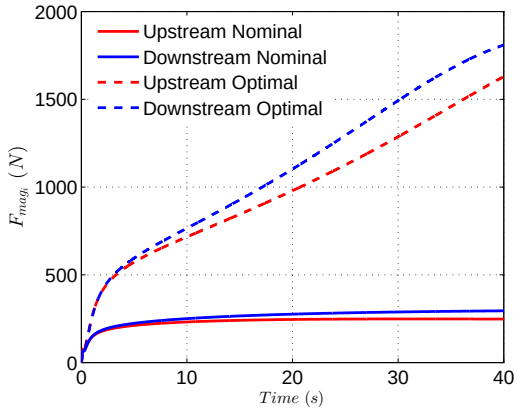

FIGURE 5. The optimal and nominal magnetic forces

Consequently, reduced amounts of energies are consumed

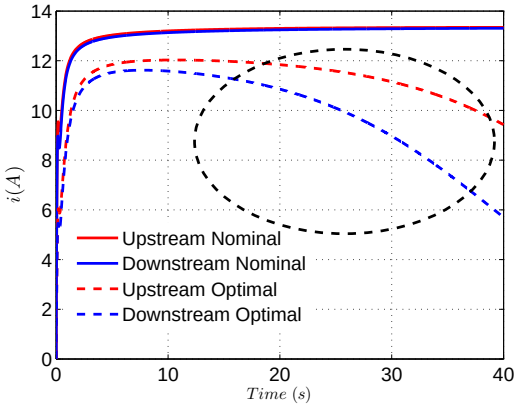

FIGURE 6. The optimal and nominal applied currents

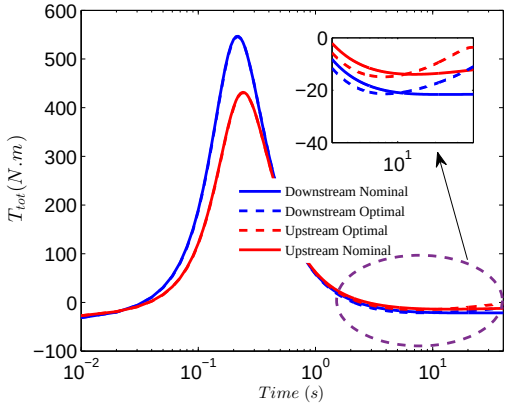

FIGURE 7. The total torques acting on both the valves

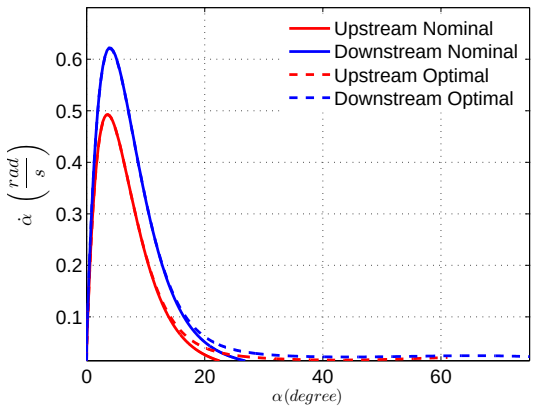

FIGURE 8. The optimal and nominal valves' rotation angles

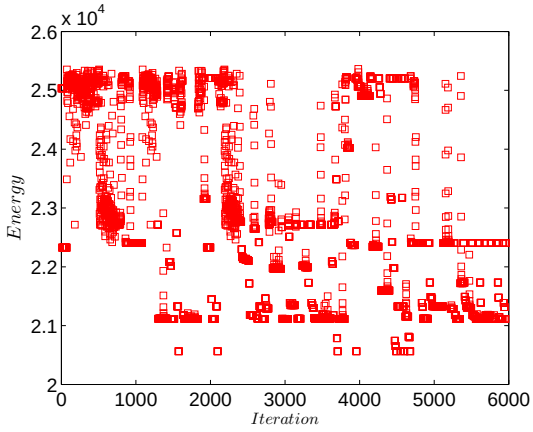

(a)

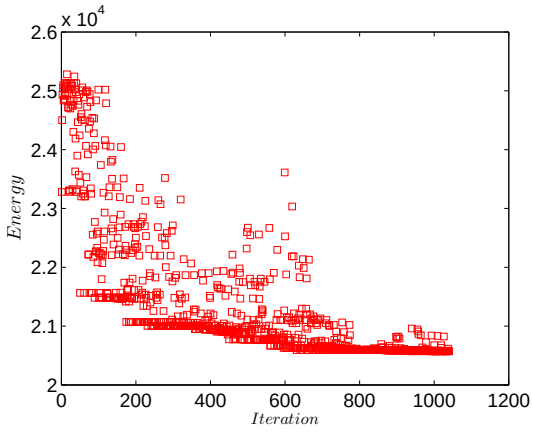

(b)

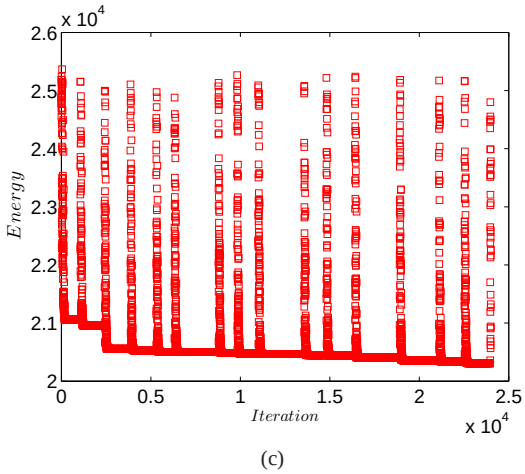

(c)

FIGURE 9. The optimized lumped amount of energy: (a) GS ($E_{opm} = 20563$; (b) GA ($E_{opm} = 20572$); (c) SA ($E_{opm} = 20400$))

as shown in Figs. 9(a), 9(b), and 9(c). Shown in Figs. 9(a), 9(b) and, 9(c) reveal upward of 18.28%, 18.25%, and 18.94% energy savings obtained through the GS, genetic, and SA algorithms, respectively, for the whole optimal systems in comparison with that of the nominal one:

$$\Delta E_{GS} = \frac{E_{nominal} - E_{optimal}}{E_{nomial}} \times 100 \approx 18.28\% \quad (40)$$

$$\Delta E_{GA} = \frac{E_{nominal} - E_{optimal}}{E_{nomial}} \times 100 \approx 18.25\% \quad (41)$$

$$\Delta E_{SA} = \frac{E_{nominal} - E_{optimal}}{E_{nomial}} \times 100 \approx 18.94\% \quad (42)$$

We repeatedly examined the optimization schemes to avoid to be trapped in local minima. The negligible difference (less than 1.6%) among the GS, genetic, and SA algorithms would potentially confirm the global minimum value. The amount of energy saved is promising in that we typically run tens of valve-actuator sets in a flow line and using such optimal configurations would help reduce the amount of energy consumption and subsequently the cost of operation for the whole network.

5 Conclusions

This paper presented a novel coupled nonlinear model of two actuators and valves subject to the sudden contraction. We discussed the effects of mutual interactions between the valves' dynamics in correlations with the flow nonlinear torques including both the hydrodynamic and bearing ones. These dependencies among different components were formalized to yield a sixth order dynamic model of the whole system. We used simulated annealing, genetic, and gradient based algorithms to carry out optimization and obtained the global minimum of the lumped cost function defined as the sum of energy consumed in each set.

The principal results of this paper can be summarized as follows.

- Energy can be saved by a remarkable amount (as much as 19%) by implementing optimal design.
- The optimal flow torques help consume a minimum level of the lumped energy.
- Lower values of the currents and subsequently instantaneous energies (by plotting $E_{ins} = v_i i_i$ vs. α_i) are consumed particularly for higher rotation angles.
- Higher values of the motive forces are obtained.
- Better optimal performances would be obtained using optimal design.

We currently focus on developing a comprehensive model for n valves and actuators to be operated optimally in series.

ACKNOWLEDGMENT

The experimental work of this research was supported by Office of Naval Research Grant (N00014/2008/1/0435).

REFERENCES

[1] Hughes, R., Balestrini, S., Kelly, K., Weston, N., and Mavris, D., 2006. "Modeling of an integrated reconfigurable intelligent system (IRIS) for ship design". In Proceedings of the 2006 ASNE Ship and Ship Systems Technology (S3T) Symposium.

[2] Lequesne, B., Henry, R., and Kamal, M., 1998. Magnavalve: a new solenoid configuration based on a spring-mass oscillatory system for engine valve actuation. GM Research Report E3-89, June.

[3] Naseradinmousavi, P., and Nataraj, C., 2011. "Nonlinear mathematical modeling of butterfly valves driven by solenoid actuators". *Journal of Applied Mathematical Modelling,* ***35***(5), pp. 2324–2335.

[4] Naseradinmousavi, P., and Nataraj, C., 2012. "Transient chaos and crisis phenomena in butterfly valves driven by solenoid actuators". *Communications in Nonlinear Science and Numerical Simulation,* ***17***(11), November, pp. 4336–4345.

[5] Naseradinmousavi, P., and Nataraj, C., 2013. "Optimal design of solenoid actuators driving butterfly valves". *ASME Journal of Mechanical Design,* ***135***(9), July.

[6] Naseradinmousavi, P., 2015. "A novel nonlinear modeling and dynamic analysis of solenoid actuated butterfly valves coupled in series". *ASME Journal of Dynamic Systems, Measurement, and Control,* ***137***(1), January.

[7] Baek-Ju, S., and Eun-Woong, L., 2005. "Optimal design and speed increasing method of solenoid actuator using a non-magnetic ring". In International Conference on Power Electronics and Drives Systems, pp. 1140 – 1145.

[8] Hameyer, K., and Nienhaus, M., 2002. "Electromagnetic actuator-current developments and examples". In 8th International Conference on New Actuators, pp. 170–175.

[9] Sung, B. J., Lee, E. W., and Kim, H. E., 2002. "Development of design program for on and off type solenoid actuator". In Proceedings of the KIEE Summer Annual Conference, Vol. B, pp. 929–931.

[10] Kajima, T., 1995. "Dynamic model of the plunger type solenoids at deenergizing state". *IEEE Transactions on Magnetics,* ***31***(3), May, pp. 2315 – 2323.

[11] Karr, C. L., and Scott, D. A., 2003. "Genetic algorithm frequency domain optimization of an anti-resonant electromechanical controller". *Lecture Notes in Computer Science*.

[12] Mahdi, S. A., 2014. "Optimization of pid controller parameters based on genetic algorithm for non-linear electromechanical actuator". *International Journal of Computer Applications,* ***94***, November.

[13] Jimenez-Octavio, J. R., Pil, E., , Lopez-Garcia, O., and Carnicero, A., 2006. "Proceedings of the 2006". In Proceedings of the 2006 Rail Conference, IEEE/ASME Joint.

[14] Nowak, L., 2010. "Optimization of the electromechanical systems on the basis of coupled field-circuit approach". *The international journal for computation and mathematics in electrical and electronic engineering,* ***20***(1), pp. 39–52.

[15] Marquardt, D., 1963. "An algorithm for least-squares estimation of nonlinear parameters". *SIAM Journal Applied Math.,* ***11***, pp. 431–441.

[16] Messine, F., Nogarede, B., , and Lagouanelle, J. L., 1998. "Optimal design of electromechanical actuators: A new method based on global optimization". *IEEE TRANSACTIONS ON MAGNETICS,* ***34***(1), pp. 299–308.

[17] Kelley, C. T., 1999. "Iterative methods for optimization". *Frontiers in Applied Mathematics,* ***18***.

[18] Sefkat, G., 2009. "The design optimization of the electromechanical actuator". *Structural and Multidisciplinary Optimization,* ***37***(6), pp. 635–644.

[19] Abergel, J., Allain, M., Michaud, H., Cueff, M., Ricart, T., Dieppedale, C., Rhun, G. L., Faralli, D., Fanget, S., and Defay, E., 2012. "Optimized gradient-free pzt thin films for micro-actuators". In 2012 IEEE International Ultrasonics Symposium (IUS), IEEE.

[20] Chakraborty, I., Trawick, D. R., Jackson, D., and Mavris, D., 2013. "Electric control surface actuator design optimization and allocation for the more electric aircraft". In 2013 Aviation Technology, Integration, and Operations Conference.

[21] Medhat, A., and Youssef, M., 2013. "Optimized pid tracking controller for piezoelectric hysteretic actuator model". *World Journal of Modelling and Simulation,* ***9***(3), pp. 223–234.

[22] Naseradinmousavi, P., 2012. "Nonlinear modeling, dynamic analysis, and optimal design and operation of electromechanical valve systems". PhD thesis, Villanova University, May.

[23] Bennett, C. O., and Myers, J. E., 1962. *Momentum, heat, and mass transfer*. McGraw-Hill.

[24] Massey, B. S., and Ward-Smith, J., 1998. *Mechanics of Fluids*, 7th ed. Taylor & Francis.

[25] Association, A. W. W., 2012. *Butterfly Valves: Torque, Head Loss, and Cavitation Analysis*, 2nd ed.

[26] Park, J. Y., and Chung, M. K., 2006. "Study on hydrodynamic torque of a butterfly valve". *Journal of Fluids Engineering,* ***128***(1), January, pp. 190–195.

[27] Leutwyler, Z., and Dalton, C., 2008. "A CFD study of the flow field, resultant force, and aerodynamic torque on a symmetric disk butterfly valve in a compressible fluid". *Journal of Pressure Vessel Technology,* ***130***(2).

[28] Naseradinmousavi, P., and Nataraj, C., 2011. "A chaotic blue sky catastrophe of butterfly valves driven by solenoid actuators". In Proceedings of the ASME 2011 International Mechanical Engineering Congress & Exposition, no. IMECE2011/62608.

[29] Kirkpatrick, S., Gelatt, C. D., and Vecchi, M. P., 1983. "Optimization by simulated annealing". *Science,* ***220***(4598), pp. 671–680.

[30] Cerny, V., 1985. "Thermodynamical approach to the traveling salesman problem: An efficient simulation algorithm". *Journal of Optimization Theory and Applications,* ***45***(1), January, pp. 41–55.

[31] H., H. J., 1975. *Adaptation in Natural and Artificial Systems*. Adaptation in Natural and Artificial Systems.